

Identification of magnetic islands in Heliotron J experiments

Yasuhiro SUZUKI^{1,2)}, Satoshi YAMAMOTO³⁾, Satoru SAKAKIBARA^{1,2)},
Hiroyuki OKADA³⁾, Kazunobu NAGASAKI³⁾, Shinji KOBAYASHI³⁾, Kiyofumi MUKAI³⁾,
Shinya WATANABE³⁾, Tohru Mizuuchi³⁾, Yoshiro NARUSHIMA^{1,2)},
Yuji NAKAMURA⁴⁾, Kiyomasa WATANABE^{1,2)} and Fumimichi SANO³⁾

¹⁾National Institute for Fusion Science, Toki 509-5292, Japan

²⁾Graduate University for Advanced Studies, SOKENDAI, Toki 509-5292, Japan

³⁾Institute of Advanced Energy, Kyoto University, Uji 611-0011, Japan

⁴⁾Graduate School of Energy Science, Kyoto University, Uji 611-0011, Japan

The equilibrium response on the magnetic island produced by external perturbed coils is studied in a Heliotron J plasma. In order to identify the equilibrium response, the magnetic diagnostic system is developed. This system consists of two parts. One is the diagnostic system based on the toroidal array of the magnetic probe. Another is a numerical code based on the 3D MHD equilibrium calculation code. Using the diagnostic system, the perturbation field driven by the equilibrium response is identified.

Keywords: magnetic island, equilibrium response, magnetic diagnostics, HINT2

1 Introduction

Generating and keeping clear flux surfaces are an aim of magnetic confinement researches, because magnetic islands and stochasticity of magnetic field leads the degradation of the confinement connecting and overlapping field lines. In tokamaks, the degradation of the confinement due to generating islands like the locked mode and neoclassical tearing mode (NTM) were observed and studied [1, 2]. The same degradations is also observed in helical system [3]. Thus, understanding and controlling of island dynamics are urgent and critical issues to aim the fusion reactor.

A method to identify magnetic islands is measuring electron temperature and density. However, if islands are rotating or healing, the profile measurement cannot identify island structure. Another method is the magnetic diagnostics. Since the magnetic diagnostics detects the change of magnetic flux directly, above problems are resolved but the diagnostics must be installed appropriately to detect perturbed field of islands.

In this study, we study island dynamics using the magnetic diagnostics in Heliotron J plasmas. Heliotron J is an $L = 1/M = 4$ helical axis heliotron configuration. A characteristic is the rotational transform profile with low magnetic shear ($\iota \sim 0.5$) to improve the particle confinement. This means there is a possibility of generating of large magnetic islands with coupling the perturbation. If low- n resonances are superposed, low- n/m islands appear. This is an advantage to study the equilibrium response on those islands. Thus, in order to generate low order magnetic islands and study the impact of the equilibrium response, external perturbation coils are designed and installed in Heliotron J device. In next section, the external

coil to produce low- n perturbation field and magnetic diagnostic system are explained. Then, first result of the island experiment is shown. Lastly, we summarize this study and show the outlook.

2 Experimental setup

2.1 Heliotron J device

The Heliotron J device is a medium sized helical-axis heliotron device ($R_0 = 1.2$ [m], $a_p = 0.17$ [m], $B_0 \leq 1.5$ [T]) with an $L = 1/M=4$ helical coil. Figure 1 shows a schematic view of the experimental system. In this experiment, the initial plasma is produced by using the second harmonic X-mode ECH (70 GHz, < 0.45 MW, non-focusing Gaussian beam) launched from a top port. To measure the perturbed field, four magnetic probes (MP01~04) are installed along the toroidal direction. These probes detect the perturbation along the toroidal direction.

2.2 Installation of external perturbation coils

The magnetic island is produced by the perturbed field from the ‘MHD instability’ and ‘MHD equilibrium response’ (equilibrium response). The identification of the perturbation on the MHD instability is easy because only detection of the perturbation from the equilibrium field is done. However, the identification of the perturbation on the equilibrium response is difficult because the equilibrium response driven by the equilibrium current (the Pfirsch-Schlüter (P-S) current, inductive and non-inductive net toroidal currents) along rippled field lines is very small. To detect the perturbation and identify the mode, the improvement of the magnetic diagnostic is necessary. As a

author's e-mail: ysuzuki@LHD.nifs.ac.jp

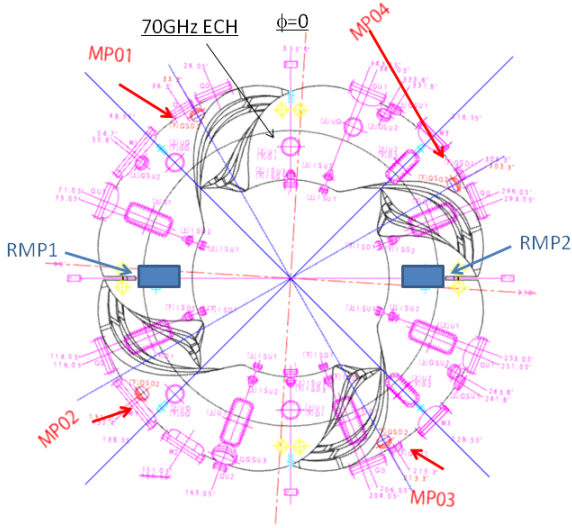


Fig. 1 Experimental setup

first step, we measure the distortion of the P-S current flow on a low- n ($n=1$) magnetic island. In theoretical analyses, spontaneous generation of the magnetic island by the equilibrium response is only for $n \geq 4$ because of $M=4$. In order to appear the distortion of the P-S current on the low- n island, the external perturbation with $n=1$ is necessary. Thus, we designed and installed two pair of resonant magnetic perturbation (RMP) coils in Heliotron J device. RMP coils to generate $n=1$ perturbation were installed at hatched positions in fig. 1. Poincaré maps of magnetic field lines are plotted at $\phi=0$. Bold lines in the figures indicate the wall of the vacuum vessel. In Fig. 1(a), an island chain by $n/m=4/8$ natural resonance appears. On the other hand, in figs.1(b) and (c), large magnetic islands with $n/m=1/2$ appear by the external perturbed field and the phase of islands is different in both cases. The external perturbed field is the quadrupole field and it is generated by two pairs of trim coils. The phase of islands can be changed by controlling the current of the trim coil. Figure 2 shows radial profiles of the rotational transform as a function of the major radius R at $\phi=0$. Although the external perturbed field is superimposed, profiles and positions of the magnetic axis are hardly changed.

3 Equilibrium response on low- n islands

Since the profile of the plasma pressure becomes flat on the island, the P-S current changes with fluttering pressure profile. The distortion of the P-S current leads the equilibrium response. The magnetic diagnostic identifies the response localized along the toroidal direction.

To study the equilibrium response due to the finite β

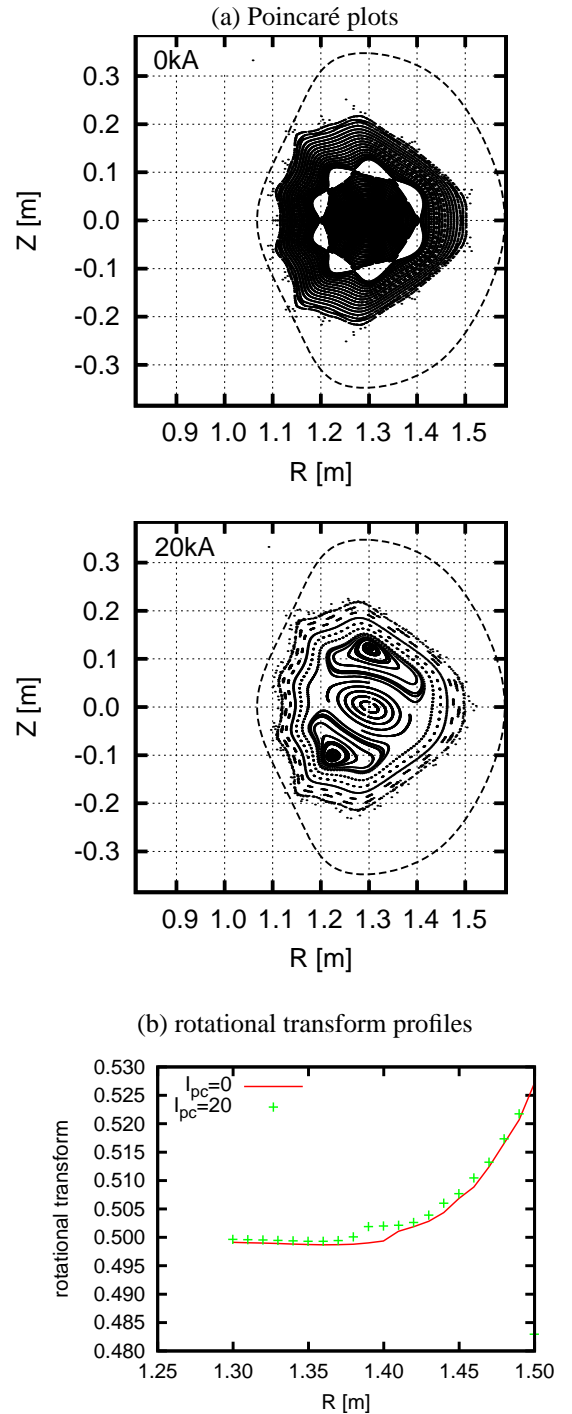


Fig. 2 Poincaré plots of magnetic field lines with and without the RMP and profiles of the rotational transform as the function of R are plotted at $\phi=\pi/4$. With the RMP, I_{RMP} is 20kA.

effect, the MHD equilibrium is calculated by the HINT2 code [4], which is a 3D MHD equilibrium solver without an assumption of nested flux surfaces *a priori*. In fig. 3, Poincaré plot of magnetic field lines and the rotational transform are shown for $\langle \beta \rangle \sim 0.2\%$ corresponding to fig. 2. For the comparison, the rotational transform for the vacuum is also shown in fig.3(b). Increased β , the rotational transform on the axis increases and the resonant surface with $n/m=1/2$ disappears. Thus, islands with $n/m=1/2$ also disappear. However, flux surfaces still distort due to external RMP field.

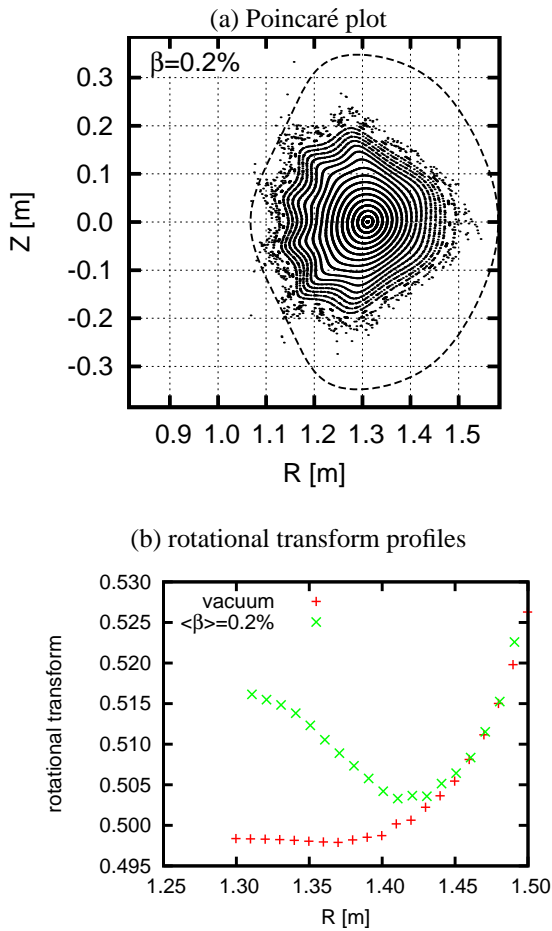


Fig. 3 Poincaré plots of magnetic field lines with and without the RMP and profiles of the rotational transform as a function of R are plotted at $\phi=\pi/4$. With the RMP, I_{RMP} is 20kA.

To identify the equilibrium response due to the finite- β effect, the pressure-induced driven by the plasma is calculated. In fig. 4, the normal component of pressure-induced field, B_n , is shown. Poloidal and toroidal angle are normalized by 2π and $\theta=0$ is the outermost position on $Z=0$ plane. The marginal difference appears along $\phi=0.9$ line. On the other hand, the poloidal component of pressure-induced field, B_θ , is plotted along the position of magnetic probes in fig. 5. the poloidal field changes along the toroidal angle ϕ . However, the change along ϕ is very small because of $\delta B_\theta < 1[G]$. Since the difference is very small,

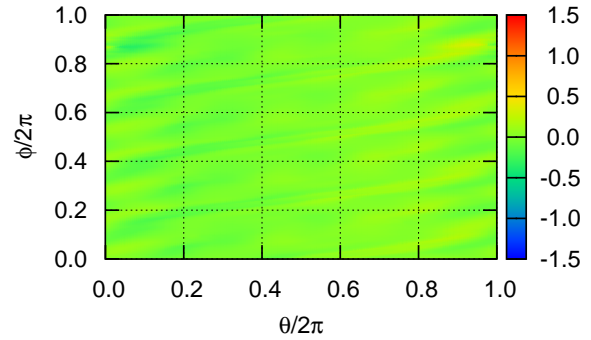


Fig. 4 The normal field component on the vacuum vessel

the observation by the magnetic probe is difficult. In order to observe significantly, the improvement of S/N ratio by the flux loop is necessary. This result will be the basis to design the flux loop in Heliotron J device.

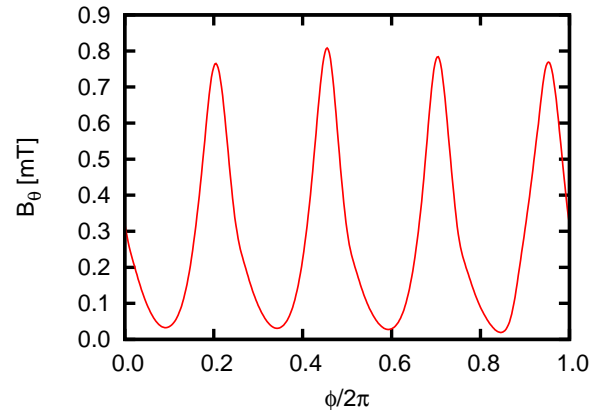


Fig. 5 The poloidal field at magnetic probes

Finally, we show the first result of the experiments with the RMP. For a typical shot (#32741) in this experiments, the density was kept $\sim 10^{19}$ and small net-toroidal current ($< 1kA$) flowed in the plasma. Unfortunately, in this experiment, the profiles of electron temperature and density could not be observed. In fig. 6, signals of magnetic probes with (#32741) or without (#32745) the RMP, respectively. Comparing fig. 6 (a) and (b), differences appeared in both cases. With the RMP, there are no signals of MP02~04. This suggests a possibility that the P-S current flow was distorted by the magnetic island and the external field driven by the P-S current was changed. However, this is still a speculation. The identification of the equilibrium response is a future subject. The signal observed by the magnetic probe was very small. Since the equilibrium response is guessed very small, the flux loop is efficient to observe small perturbation field. The design of flux loop to Heliotron J device is another future subject.

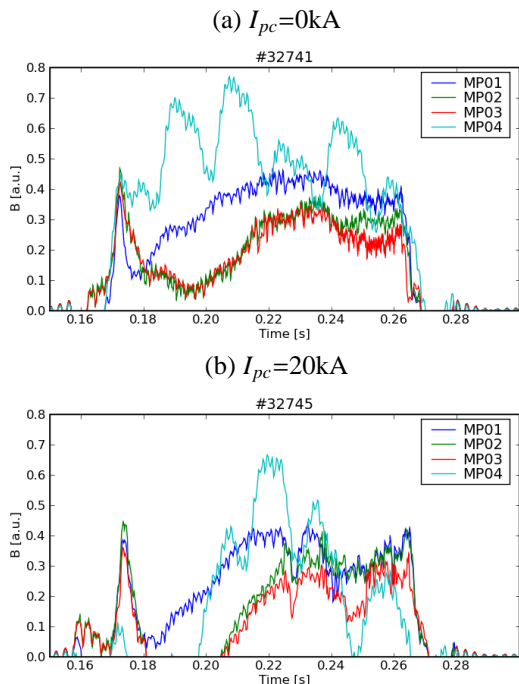


Fig. 6 Signals of magnetic probes in two shot (no RMP and RMP). With the RMP, I_{RMP} is 20kA.

4 Summary

we designed and installed external RMP coils to Heliotron J device. These coils can produce low- n magnetic island in the plasma. To detect the distortion of the equilibrium current flow by large magnetic islands, we can study the effect of the equilibrium response on the spontaneous changing magnetic islands. We also show the first result of the configuration with the RMP field. The difference on signals of magnetic probes appeared by superposing the RMP field.

Acknowledgements

The authors thank the Heliotron J staff for conducting the experiments and discussions. This work was supported by NIFS/NINS under the NIFS Collaborative Research Program (NIFS07KOAP018, NIFS07KUHL011, NIFS07KUHL016, NIFS06KTAT023, NIFS07KNXN104) This work was partly supported by Grant-in-Aid for Scientific Research from the Japan Society for the Promotion of Science No. 17206094, 19360419 and 20760585.

- [1] J. A. Snipes, D. J. Campbell, P. S. Haynes et al., Nucl. Fusion **28**, 1085 (1988)
- [2] R. Carrera, R. D. Hazeltine, and M. Kostchenreuther, Phys. Fluids **29**, 899 (1986)
- [3] N. Ohyabu et al., Phys. Rev. Lett. **97**, 055002 (2006)
- [4] Y. Suzuki et al., Nucl. Fusion. **46**, L19 (2006)